

Figure S1. **c-Src mediates FHL1 phosphorylation at Tyr149 and Tyr272.** (A) Amino acid sequence of human FHL1 showing four putative tyrosine phosphorylation sites, Tyr117, Tyr149, Tyr213, and Tyr272, detected by mass spectrometry. (B and C) Tandem mass spectrometry spectra and sequence coverage (y and b ions) for the FHL1 phosphopeptides GEDFY<sup>P</sup>CVTCHETK and FVFHQEQVY<sup>P</sup>CPDCAK derived from FHL1 coexpressed with c-Src in HeLa cells.

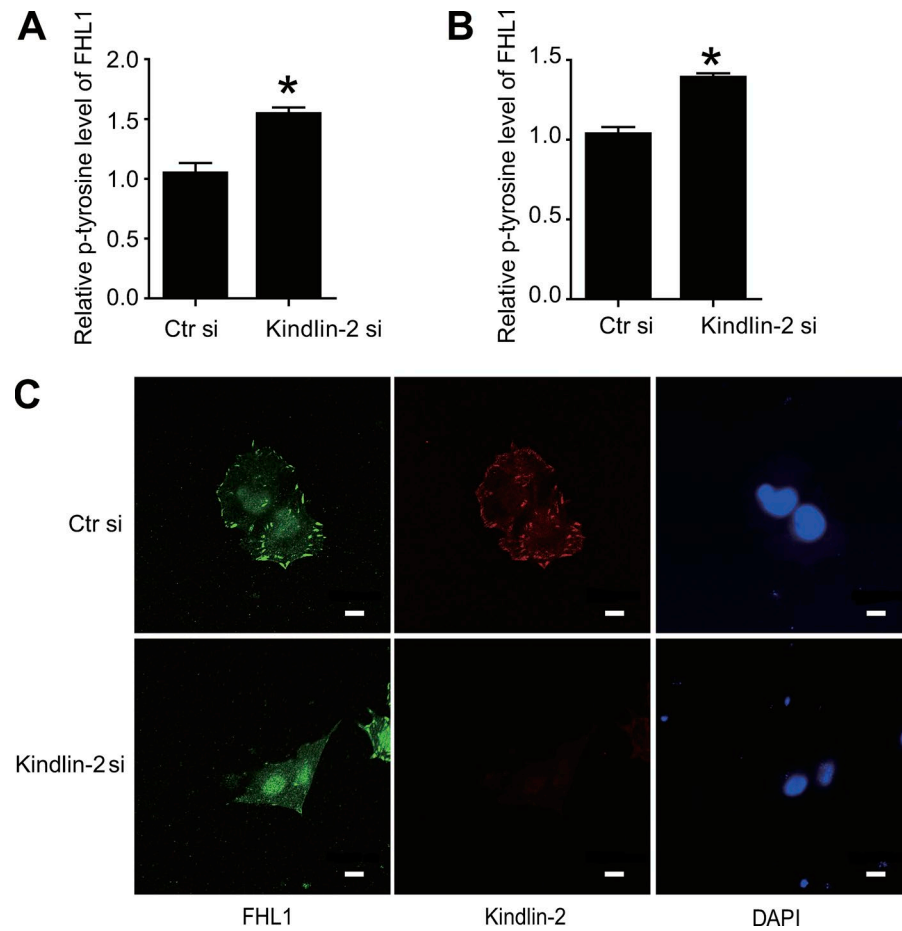


Figure S2. **Statistical analysis of Fig. 4 (D and E) and subcellular localization of FHL1 regulated by kindlin-2.** (A) Statistical analysis of Fig. 4 D. p-Tyr levels of FHL1 were detected in H1299 cells transfected with control siRNA or kindlin-2 siRNA for 48 h. (B) Statistical analysis of Fig. 4 E. HeLa cells were transfected with indicated plasmids, and siRNAs and p-Tyr levels of FHL1 were detected. The intensity of the p-Tyr bands from the FHL1 IP from three separate biological replicates was quantified and statistically analyzed by two-tailed Student's *t* tests. \*,  $P < 0.05$ . (C) H1299 cells transfected with the control siRNA or kindlin-2 siRNA were replated on FN-coated coverslips for 4 h and stained with anti-kindlin-2 and anti-FHL1 antibodies. The nuclei were stained with DAPI. Bars, 10  $\mu$ m.

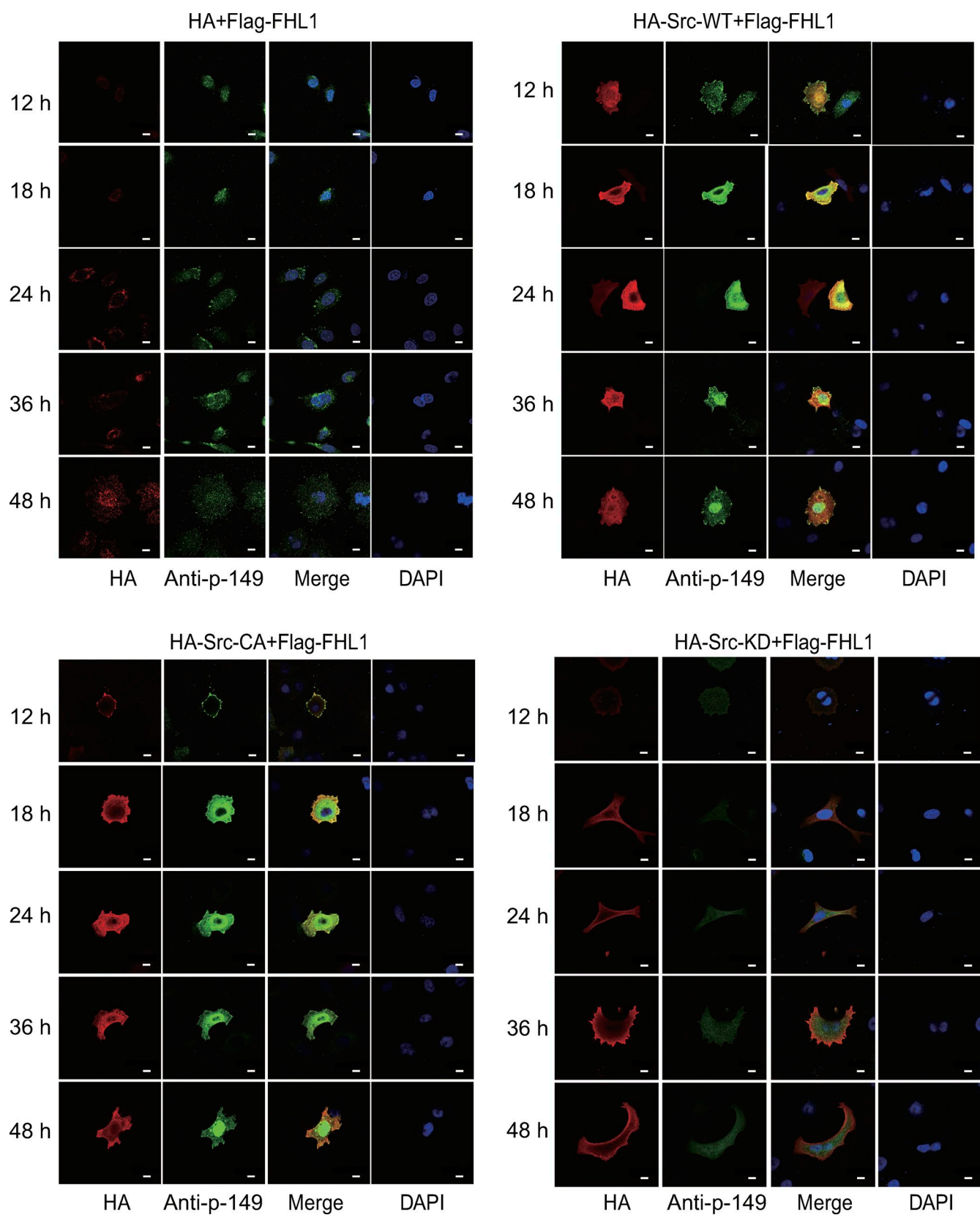


Figure S3. **Time series of FHL1 phosphorylation induced by Src.** HeLa cells transfected with different constructs of Src for different time were replated on FN-coated coverslips for 4 h and stained with anti-HA and anti-p-FHL1 antibodies. The nuclei were stained with DAPI. Bars, 10  $\mu$ m.

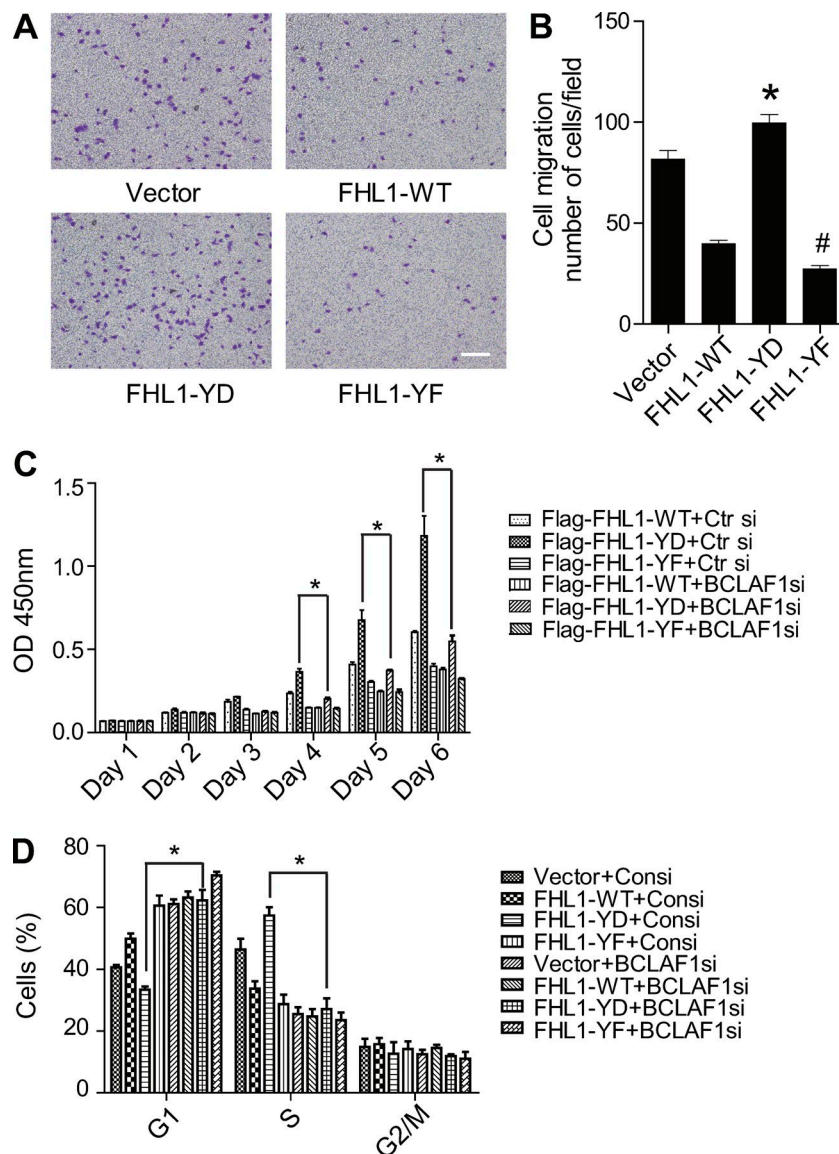


Figure S4. **FHL1 phosphorylation promotes lung cancer cell migration and statistical analysis of Fig. 7 (H and J).** (A and B) H1299 cells stably expressing FHL1-WT, FHL1-Y149-272D (FHL1-YD), and FHL1-Y149-272F (FHL1-YF) were established, and a transwell assay was performed to examine the effect of FHL1 phosphorylation on H1299 cell migration. Bar, 50  $\mu$ m. \*,  $P < 0.05$  versus vector group; #,  $P < 0.05$  versus FHL1-Y149-272D. (C) A WST1 assay was performed when BCLAF1 was knocked down in H1299 cells stably expressing FHL1-WT, FHL1-Y149-272D, and FHL1-Y149-272F mutants. (D) Effect of BCLAF1 depletion by siRNA on the distribution of the cell cycle of H1299 cells analyzed by flow cytometry. Statistical analyses were performed by one-way ANOVAs. Values shown are means  $\pm$  SD of triplicate measurements. \*,  $P < 0.05$ .



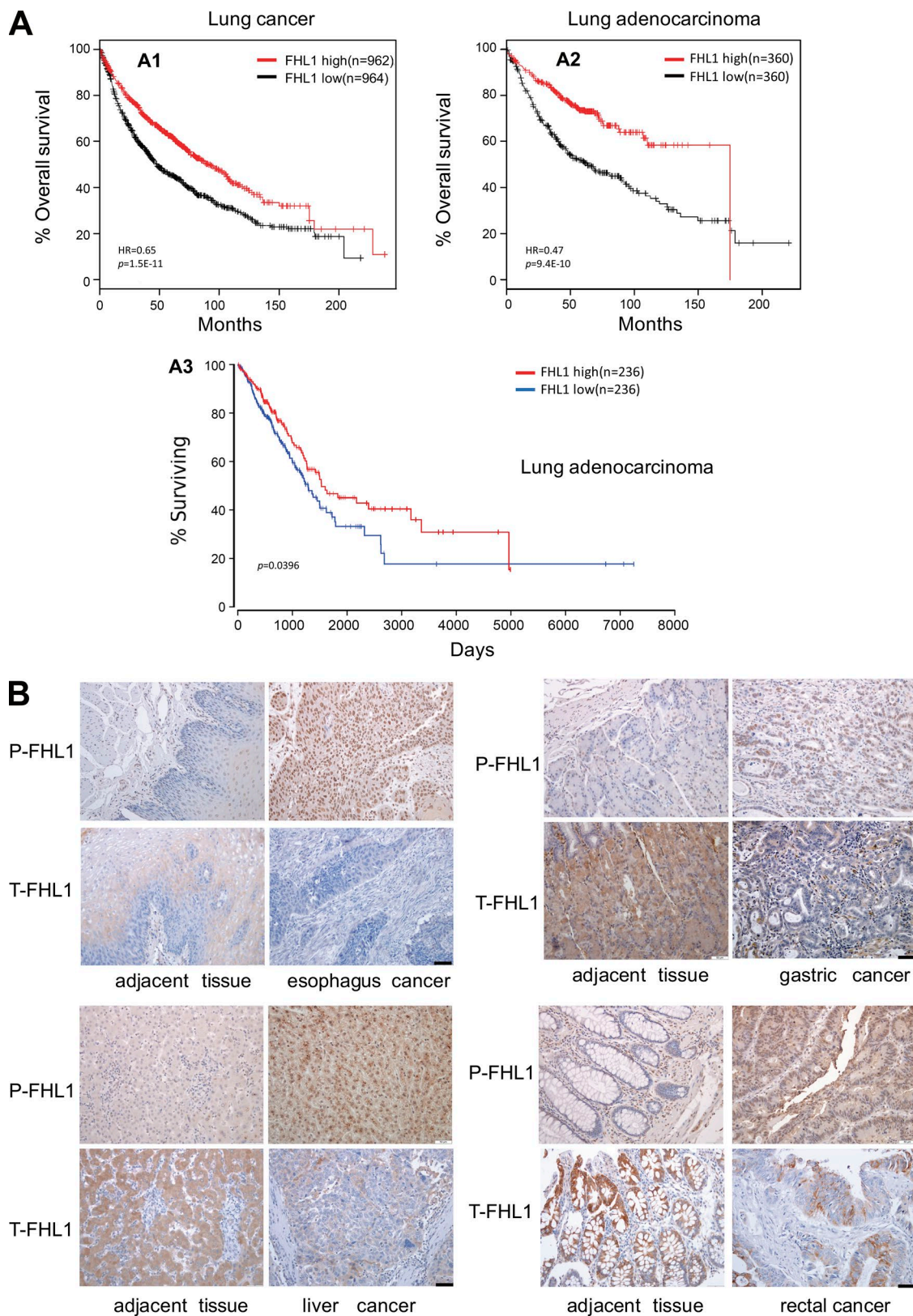


Figure S5. **Analysis of FHL1 expression by databases and tissue chips.** (A) Data of FHL1 expression were analyzed by the Kaplan-Meier Plotter analysis database (A1 and A2) and the TCGA database (A3). HR, hazard ratio. (B) Phosphorylation of FHL1 and total FHL1 expression in tissue chips of multiple organ cancer was determined by immunohistochemistry using anti-p-FHL1 or anti-FHL1 antibodies. The images of liver cancer, gastric cancer, rectal cancer, and esophagus cancer are shown. Bars, 50  $\mu$ m.

**Table S1** is a separate Excel file showing mass spectrometry spectra analysis of the **FHL1** interaction with **BCAFL1** in the nucleus.